Chapter 2

Coding Metasurfaces and Applications

Hengyi Sun, Changqing Gu, Zhuo Li and Ferran Martin

Additional information is available at the end of the chapter

http://dx.doi.org/10.5772/intechopen.78417

Abstract

Metasurfaces are the planar counterparts of metamaterials, and they consist of a single-layer or a few-layers stack of planar structures, which can be fabricated using lithography and nanoprinting methods. Such artificial structures are usually described by effective medium parameters at the macroscopic scale. In this chapter, we deal with "coding metasurfaces," composed of only two types of unit cells, with 0 and π phase responses, from which electromagnetic (EM) waves can be manipulated and different functionalities can be realized. We review the recent progress in the physics of metasurfaces operating at wavelengths ranging from microwave to visible. We provide an overview of key metasurface concepts, such as diffusion, anomalous reflection and refraction, and introduce metasurfaces based on some optimization methods to design metasurfaces, as well as their use in wave-front shaping and beam-forming applications, followed by a discussion of polarization conversion in few-layer metasurfaces and their related properties. An overview of diffusion coding metasurface reveals their ability to realize unique functionalities to reduce the radar cross-section (RCS). We also describe diffusion coding metasurfaces that can improve the field uniformity in reverberation chambers. Finally, we conclude by providing our opinions on opportunities and challenges in this rapidly developing research field.

Keywords: coding, metasurface, metamaterial, broadband, diffusion

1. Introduction

Recently, the ability to manipulate the electromagnetic (EM) waves has been significantly improved with the help of the emerging concept of metasurface. Driven by the seminal

work by Yu et al. [1], metasurfaces have gained considerable attention, and nowadays constitute one of the most promising research thrusts in the field of artificial materials. Della Giovampaola and Engheta presented a method for constructing "metamaterial bytes" through proper spatial mixtures of "digital metamaterial bits" [2] in which the "digital metamaterial bits" are some particles that possess distinct material properties. However, the resulting metamaterial bytes are still described by the effective medium parameters. Cui proposed the general concepts of "coding metamaterial," "digital metamaterial," and "programmable metamaterial," which means that a single metamaterial can be digitally controlled to obtain distinctly different functionalities [3, 4]. Two types of unit cells with 0 and π phase responses to mimic the "0" and "1" elements were proposed for 1-bit digital metamaterial such that they can be controlled using existing digital technology. By designing coding sequences of "0" and "1" elements in coding metamaterials, EM waves can be easily manipulated to obtain different functionalities. And this concept can also be extended to 2-bit (0, $\pi/2$, π, and $3\pi/2$) and 3-bit (0, $\pi/8$, $\pi/4$, $3\pi/8$, $\pi/2$, $5\pi/8$, $3\pi/4$, and $7\pi/8$) or more. We will start this chapter by designing a 1-bit coding metasurfaces, which are useful to achieve radar cross-section (RCS) reduction, polarization conversion, anomalous reflection, and vortex beam reflection. By investigating the scattering characteristic of the coding metasurface, we replace the stirrer of a reverberation chamber (RC) with a diffusion coding metasurface in order to improve the field uniformity of the RC, in the meanwhile, increasing the test area of the RC, making the application of the metasurfaces extended to the electromagnetic compatibility (EMC) area.

2. Coding metasurface

By using coding metasurfaces with two basic unit cells with out-of-phase responses, diffuse scattering has been achieved. Applications are as diverse as radar signature control and computational imaging, among others [3]. Of specific interest for the present study is the concept of "coding and digital" metasurfaces, recently put forward by Cui et al. [4]. We will not go deep into the physical details of such procedure since this is not the aim of this chapter and the topic is clearly treated in Ref. [4]. We will simply illustrate the application of the concept using coding metasurface examples.

2.1. RCS reduction

In general, the unit cell structure of a specific metasurface exhibits different phase responses under normal incidence (along with the *z*-direction) depending on the rotation angle in the xy-plane [5]. The unit cell structures and its reflection characteristics are illustrated in **Figure 1**.

Two structures with relative phase responses of π can be arranged in a chessboard-like metasurface to reduce the RCS under monostatic backscattering conditions. The simplest method of constructing an RCS-reducing metasurface using 1-bit unit cells is to generate a phase distribution matrix with "0" and "1" elements randomly distributed, and place each element according to its reflection phase. According to array theory, the lattice scattered electric-field intensity in the far-field region can be expressed as:

http://dx.doi.org/10.5772/intechopen.78417

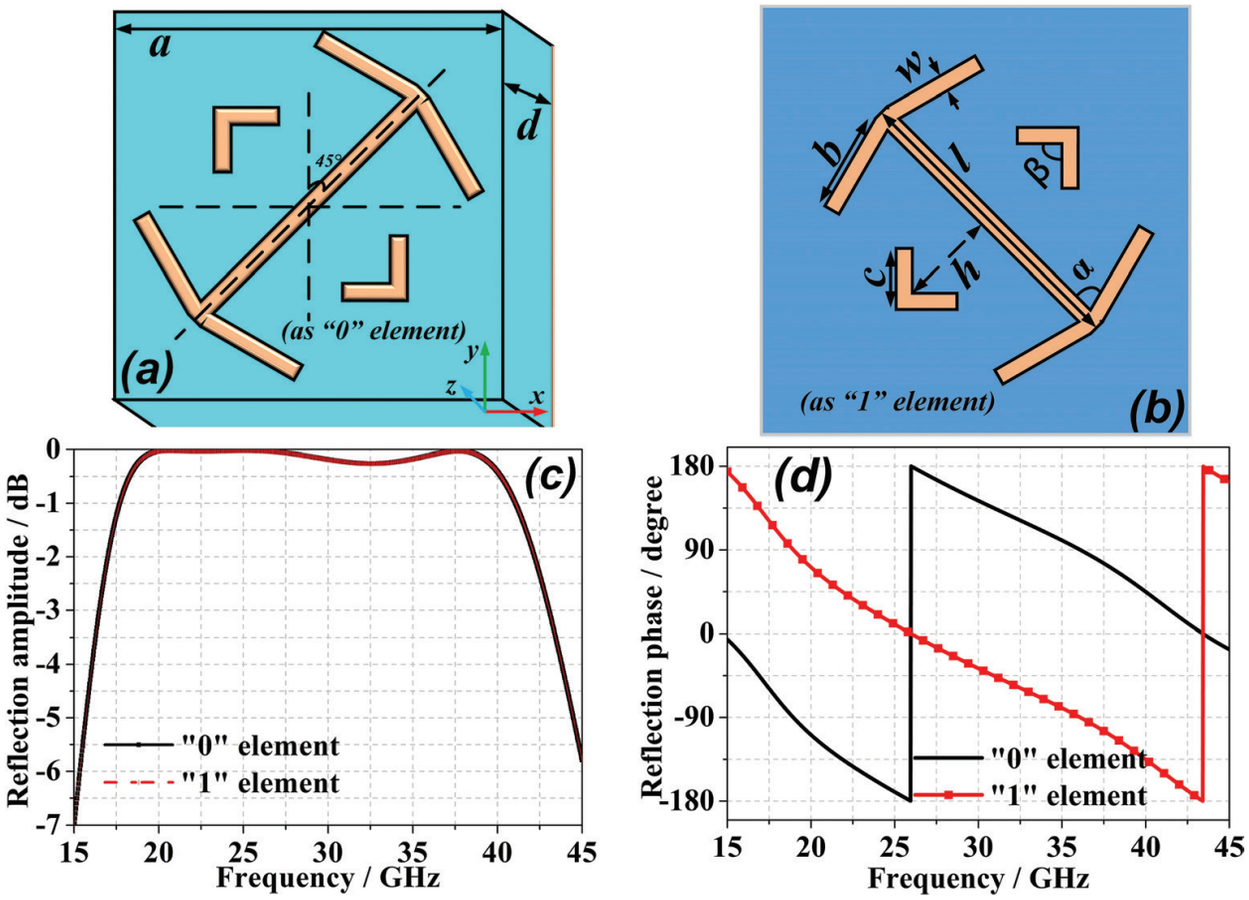

Figure 1. Front views of "0" and "1" element unit cells. The unit cell structure with an angle of 45° to the y-axis represents the "0" element (a), and the structure rotated 90° counter-clockwise about the z-axis is the "1" element (b). Reflection properties of "0" and "1" elements versus frequency under normal x-polarized electromagnetic incident waves: (c) lattice reflection amplitudes; and (d) lattice reflection phases. Reprinted with permission from Ref. [5]; Copyright 2017 Scientific Reports.

$$E_{m,n} = \frac{K_{m,n} A_{m,n} \exp\left(j \Phi_{m,n}\right) f_{m,n}(\theta, \varphi)\left(\exp\left(-jk_0 r_{m,n}\right)\right)}{r_{m,n}} \tag{1}$$

where $\boldsymbol{K}_{\mathbf{m,n}}$ is the scale coefficient, $\boldsymbol{r}_{\mathbf{m,n}}$ is the distance between the lattice point (m, n) and the far-field region observation point, and $\boldsymbol{f}_{\mathbf{m,n}}\boldsymbol{(\theta, \phi)}$ is the lattice scattering pattern function, given with respect to the elevation and azimuth angles $\boldsymbol{\theta}$ and $\boldsymbol{\phi}$. Moreover, $\boldsymbol{A}_{\mathbf{m,n}}$ and $\boldsymbol{\Phi}_{\mathbf{m,n}}$ are the lattice reflection amplitude and phase coefficient, respectively. After using an optimization algorithm to design, the entire coding metasurface is shown in **Figure 2**. Both the simulation and experimental results demonstrate that the optimal random coding metasurface can efficiently realize broadband RCS reduction more than 10 dB from 17 to 42 GHz when the angle of incident waves varies from 10 to 50°. The characteristic of broad bandwidth and broad-angle of incident waves for RCS reduction makes it promising for electromagnetic cloaking in microwave regime (as shown in **Figures 3** and **4**).

2.2. Linear polarization conversion

Polarization converters are usually designed using twisted nematic liquid crystals based on the Faraday Effect. To broaden polarization conversion bandwidth, stacked multilayer

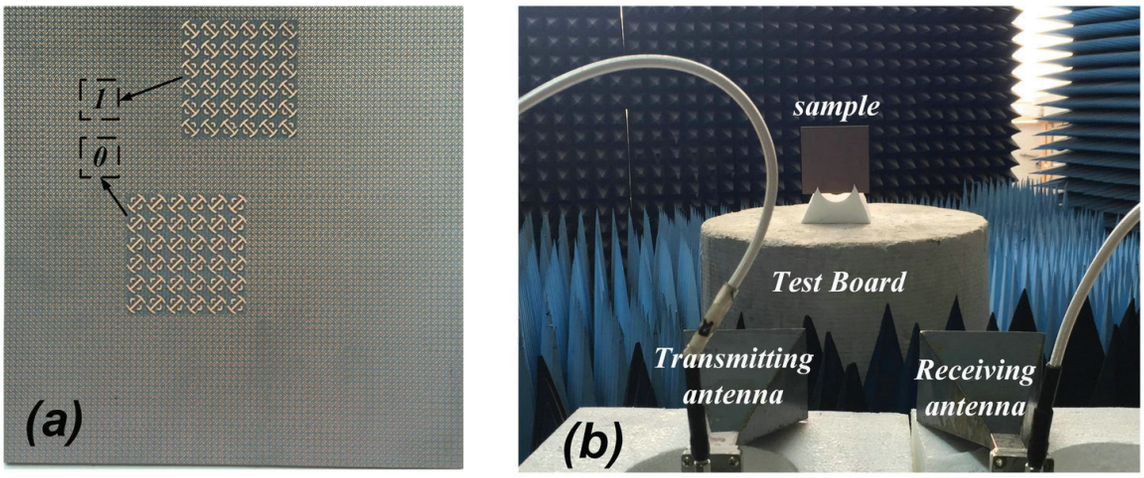

Figure 2. The optimized 1-bit coding metasurface of planform obtained after optimization. The "0" and "1" lattices comprise 6 × 6 equivalent unit cells. (a) The fabricated 1-bit GA-optimized coding metasurface. (b) The experimental setup for verifying RCS reduction. Reprinted with permission from Ref. [5]; Copyright 2017 Scientific Reports.

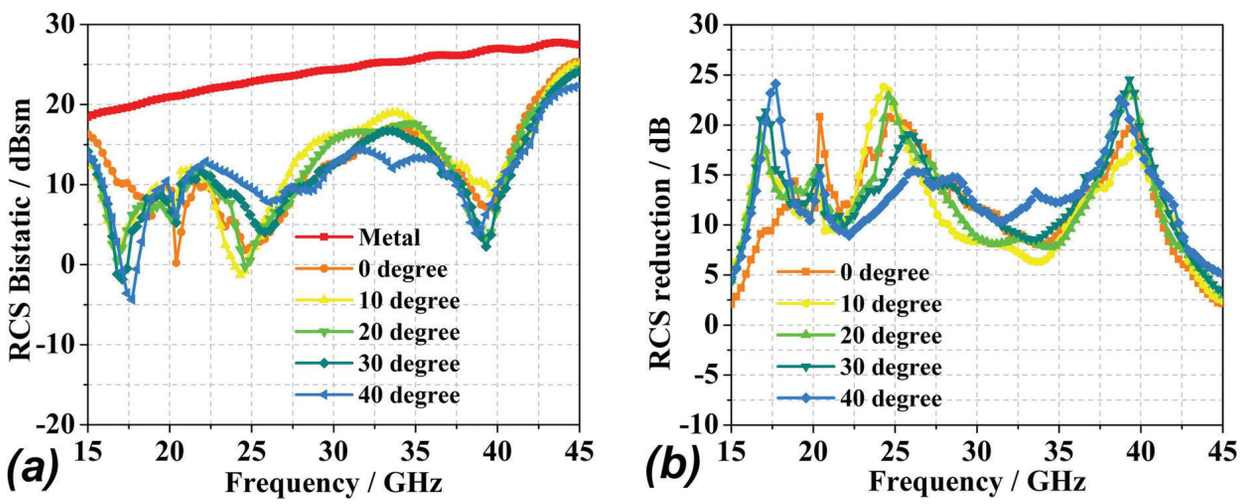

Figure 3. RCS of the metal and optimized coding metasurface under obliquely incident electromagnetic waves from 10 to 40° in simulation: (a) bistatic RCS; (b) RCS reduction. Reprinted with permission from Ref. [5]; Copyright 2017 Scientific Reports.

structures can be used. Based on changing the dimension and geometry of the unit cells of the metasurface, an ultra-wideband linear polarization rotator designed by combining three typical symmetry-broken structures, a double-head arrow, a cut-wire, and two short V-shaped wire resonators has been presented [6]. The asymmetric structure of the unit cell of the periodic array is homogeneous and anisotropic, with dispersive relative permittivity and permeability. For a plane wave (PW) with the specified polarization impinging on the artificial electromagnetic metasurface, both x- and y-polarization EM waves can be generated by reflection and transmission due to the anisotropic characteristics of the metasurface. The waves experience multiple reflections between the artificial metallic structure and the metallic sheet layer, so that the final reflected waves are a result of an interfering wave phenomenon. To better understand the multiple resonances of the structure, the incident EM wave

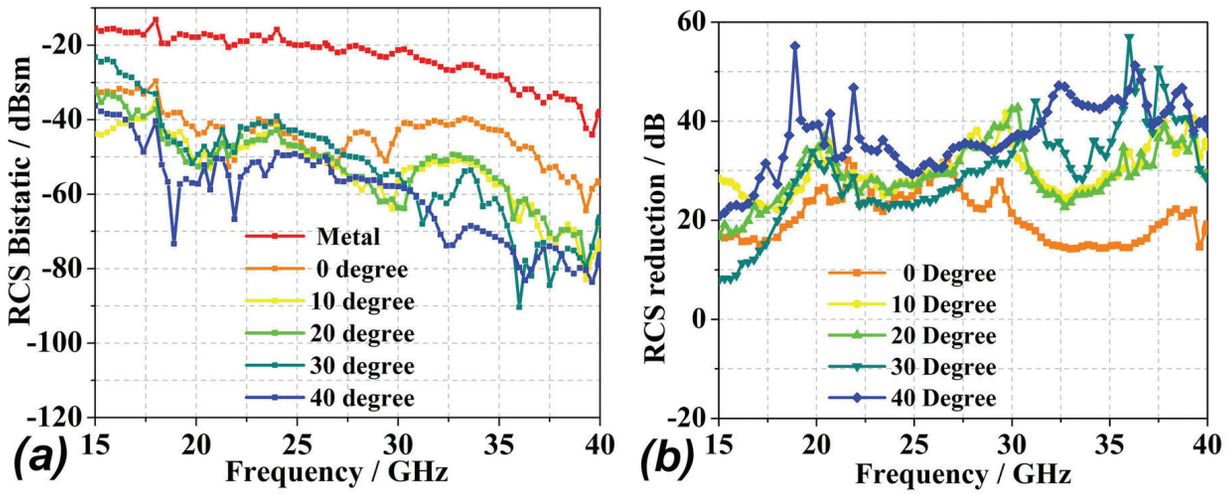

Figure 4. The experimentally obtained RCS (a) and RCS reduction (b) for various incident angles with vertical polarization. Reprinted with permission from Ref. [5]; Copyright 2017 Scientific Reports.

polarization direction is considered to be along the y-axis. Therefore, it can be decomposed into two perpendicular components u and v (see **Figure 5(b)**). Hence, the incident EM wave can be expressed as:

$$\vec{E}_i = \vec{u}\, E_{iu}\, e^{j\phi} + \vec{v}\, E_{iv}\, e^{j\phi} \tag{2}$$

Whereas the reflected wave can be written as:

$$\vec{E}_r = \tilde{r}_u \vec{u}\, E_{iu}\, e^{j\phi} + \tilde{r}_v \vec{v}\, E_{iv}\, e^{j\phi} \tag{3}$$

Where $\tilde{r}_u$ and $\tilde{r}_v$ are the reflection coefficients along u- and v-axis, respectively.

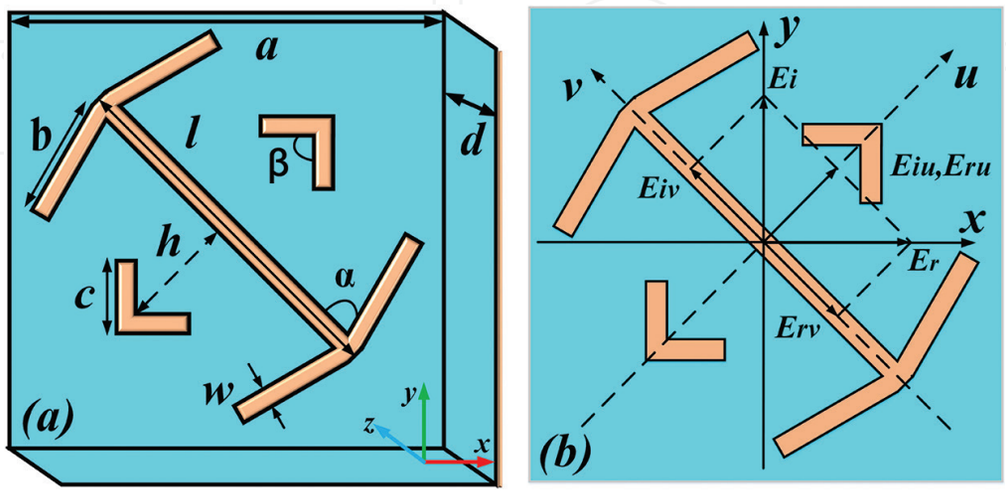

Figure 5. (a) Front view of the metasurface unit cell. (b) Intuitive scheme of y- to x-polarization conversion of the metasurface. Reprinted with permission from Ref. [6]; Copyright 2017 Journal of Applied Physics.

When arbitrarily polarized EM waves are incident, three resonances can be excited in general since both v- and u-components exist simultaneously. The superposed contributions from two individual orthogonal electric components excite independently the corresponding resonance eigenmodes. **Figure 6** shows that two eigenmodes are excited in the v-polarized case, and one eigenmode is excited in the u-polarized case.

Due to the presence of three resonances, cross-polarization reflection bandwidth can be expanded significantly. As an explicit example, simulation and measurement results show that the proposed metasurface can convert linear polarized EM waves into cross-polarized waves with polarization conversion ratios (PCR) higher than 90% from 17.3 to 42.2 GHz.

2.3. Anomalous reflection

Phase gradient metasurface (PGM) is a new way to control reflected beams. In particular, the anomalous reflection and refraction can be achieved using a PGM, by properly designing the unit cells phase gradient of the metasurface [7]. With a PGM negative refraction/reflection can be easily achieved. Because of the singular properties of the PGM, the generalized Snell's law is established. Although the PGM has many relevant features, it is not easy to design. To obtain the high efficient PGM, the adjacent unit cells of the metasurface must meet the same scattering amplitude and strict scattering phase gradient. Fortunately, the unit cell of the metasurface is placed on the front of the sheet metal, and the reflection amplitude of each unit cell is almost equal. Therefore, it is relatively easy to design the PGM, since we only need to consider the phase gradient design. By taking advantage of this concept, we designed a reflective PGM with a center frequency of 3 GHz using arc-cross shaped structure (**Figure 7**).

By changing the parameters of the metal structure, seven-unit-cell structures with a stable phase difference and a phase distribution covering 2π are selected for the periodic arrangement. An excitation port is provided 150 mm away from the metasurface in the Z-direction. The direction of the impinging wave electric field is along the $\phi = 45°$ on the XOY plane and

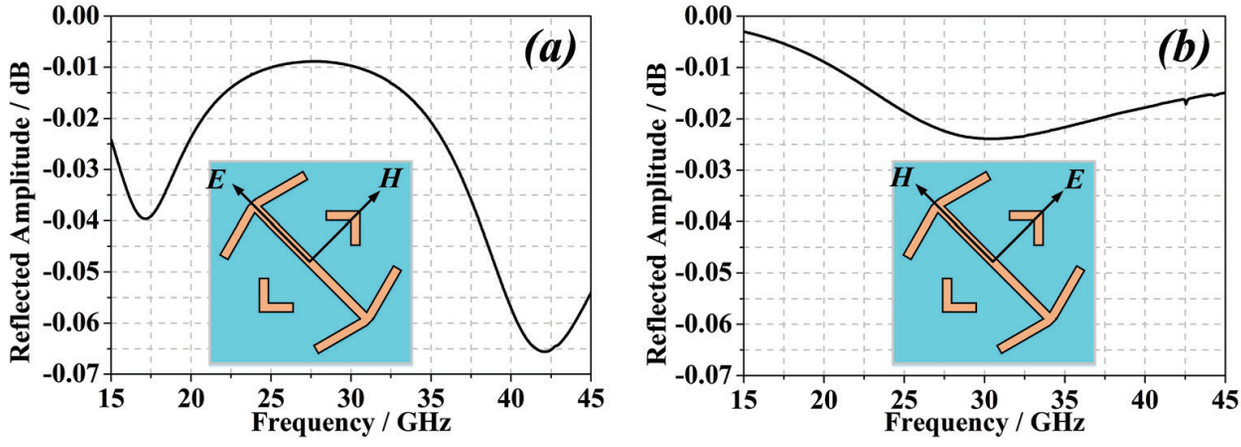

Figure 6. The three eigenmodes of the unit cell under normal incidence: (a) v-polarized, (b) u-polarized. Reprinted with permission from Ref. [6]; Copyright 2017 Journal of Applied Physics.

http://dx.doi.org/10.5772/intechopen.78417

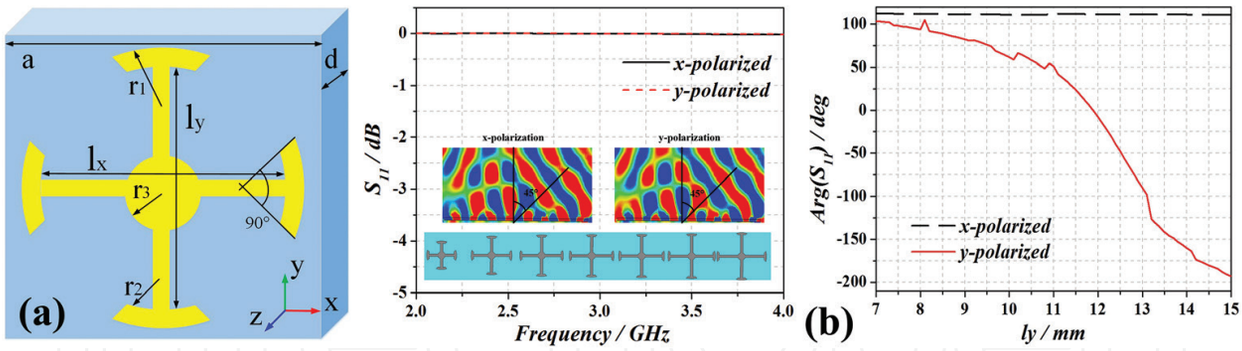

Figure 7. (a) The front view of the unit cell. (b) The simulation results of the unit cell reflection amplitude (left) and phase (right) under x-polarized and y-polarized incident EM waves. Reprinted with permission from Ref. [7]; Copyright 2016 IEEE.

the incident wave is incident along the z-direction. Since the polarization direction of the electromagnetic wave can be seen as the synthesis of vectors of x-polarization and y-polarization, the results show that the high-efficiency anomalous reflection metasurface (at 3GHz) provides 45° angle of reflection, and the reflection efficiency is above 90%. The anomalous reflection metasurface has features such as light weight, small size, and wide frequency band, which has a certain application prospect in invisible and communication fields.

2.4. Vortex beam

Since Allen indicated electromagnetic waves carrying orbital angular momentum (OAM), a variety of studies on OAM have intensively stepped into the domain of optics for its obvious advantages. OAM has been widely applied in optics, while the researches of OAM in radio frequencies have moved slowly for a long time. Metasurfaces are extraordinarily promising because of their unprecedented capability of modulating wavefronts of electromagnetic waves and their thin structures, which was first used to generate optical vortices based on the generalized laws of reflection and refraction. Although fruitful progress has been achieved toward OAM across both optical and radio frequency domains, vortex wave generation are mostly limited to a narrow frequency band. An efficient and simple reflective metasurface array that can generate vortex wave with arbitrary single-mode in ultra-wideband from 18 to 42 GHz has been designed [8] (as shown in **Figure 8**).

Though the unit cells are uniformly distributed on the roundel, the electric fields (E-fields) reflected by different cell structures are different. By observing the phase wavefront variation at different frequencies, **Figure 9** shows that the operational bandwidth of the proposed reflective metasurface for vortex wave generating is about from 18 to 42 GHz with the desired vortex wave with a mode of $l = 1$.

The proposed approach generates one vortex wave for a given structure. With future improvement, the metasurface can also be designed with multiple concentric rings, each containing a self-arranged arrow-shaped array. It is then possible to use only one structure to selectively generate different vortex waves. **Figure 10** shows the configuration of the designed vortex metasurface with multiple-modal.

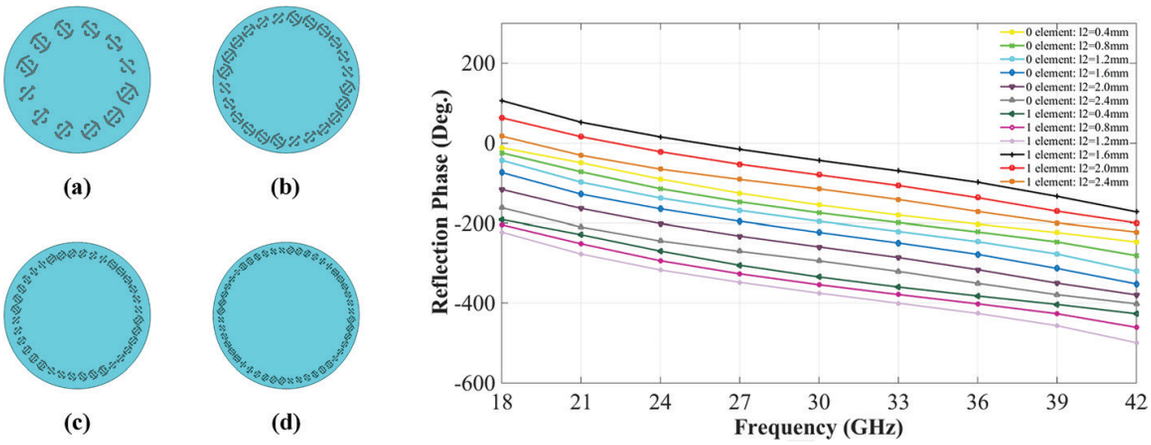

Figure 8. Configuration of the designed vortex metasurface with mode (a) $l = 1$ (b) $l = 2$ (c) $l = 3$ (d) $l = 4$ panel present the metallic patterns of the top layer. The phase of the reflection coefficient versus the length of the arrow-shaped metasurface from 18 to 42 GHz. Reprinted with permission from Ref. [8]; Copyright 2018 IEEE.

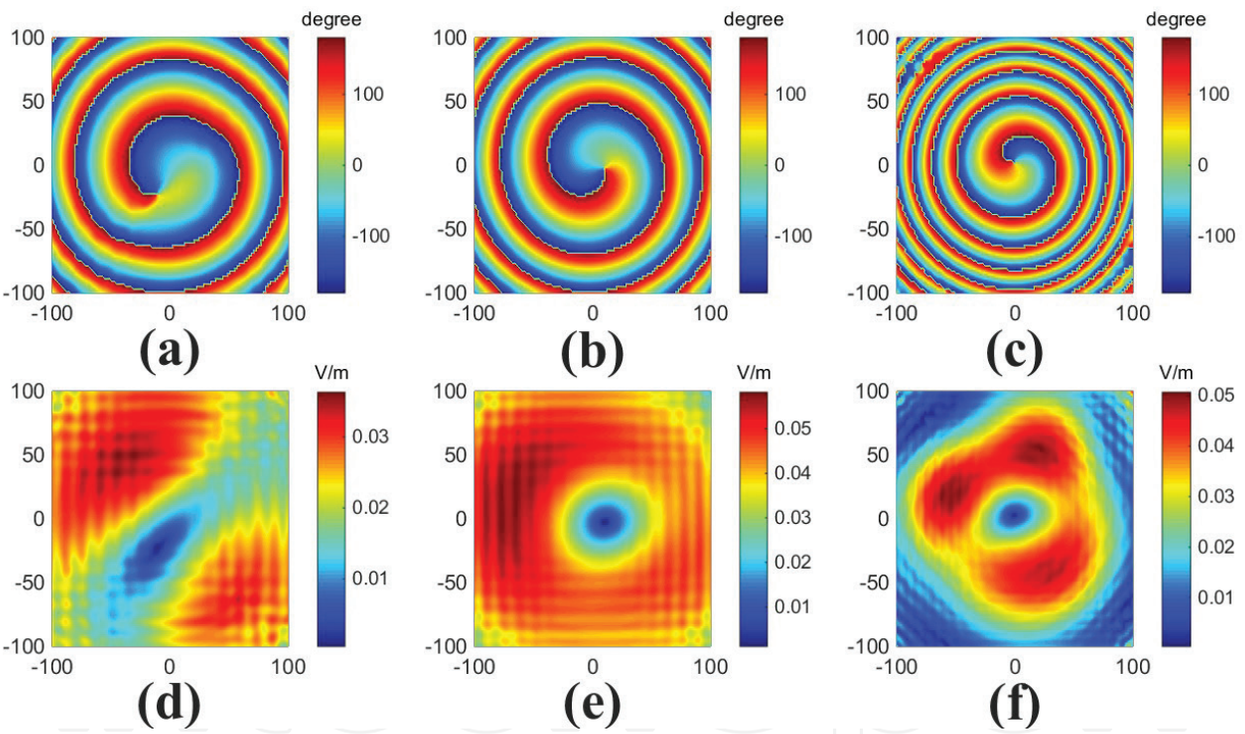

Figure 9. Phase distribution of E-filed on the observation plane at z-axis direction with mode $l = 1$ (a) at 18 GHz, (b) at 30 GHz and (c) at 42 GHz and corresponding magnitude distribution with mode $l = 1$ (d) at 18 GHz, (e) at 30 GHz, and (f) at 42 GHz. Reprinted with permission from Ref. [8]; Copyright 2018 IEEE.

Since information can be encoded as OAM states that span a much larger space than three-state OAM, the proposed configuration may provide an effective way to generate vortex waves for wireless communication applications, which will greatly promote the study and application of vortex wave. Comparing to the published work, which only can generate one OAM modal, the proposed reflective metasurface is likely to double the information rate.

http://dx.doi.org/10.5772/intechopen.78417

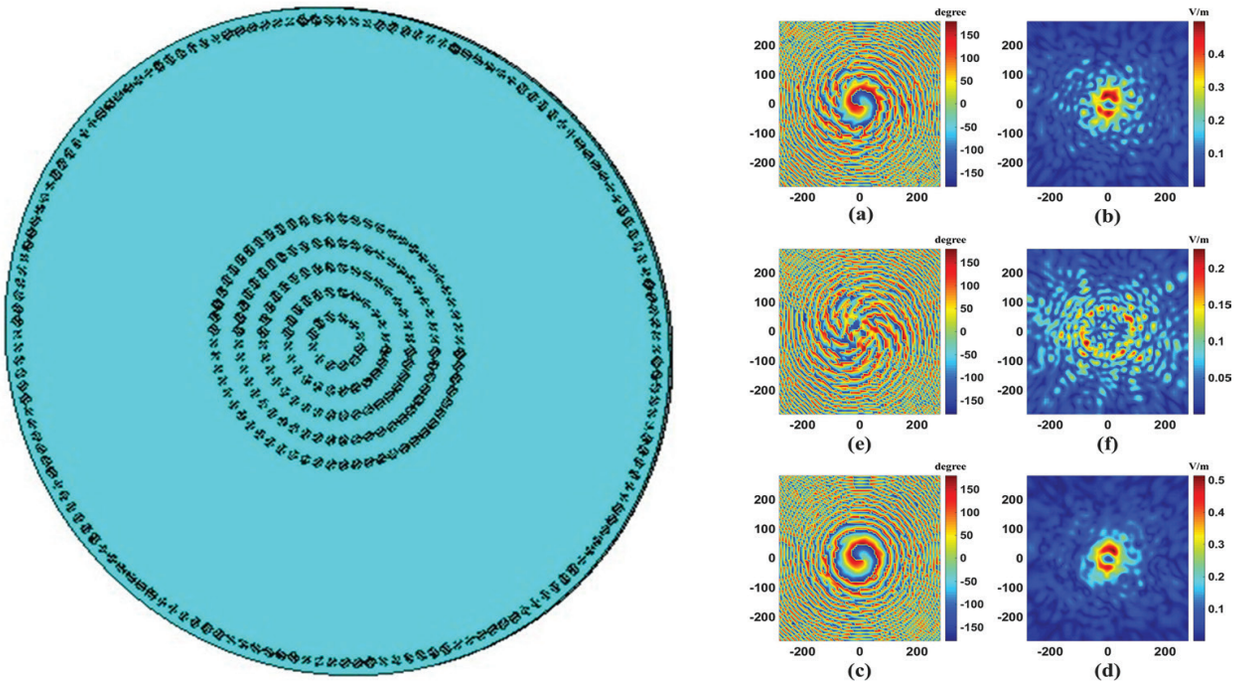

Figure 10. Configuration of the designed vortex metasurface with multiple-modal l = 1 and l = 13. Phase distribution of E-filed on the observation plane at z-axis direction with multi-modal l = 1 and l = 13 (a) at 18 GHz, (c) at 30 GHz, (e) at 42 GHz and corresponding magnitude distribution (b) at 18 GHz, (d) at 30 GHz, and (f) at 42 GHz. Reprinted with permission from Ref. [8]; Copyright 2018 IEEE.

3. The application of the coding metasurface in RC

In general, the RC is rectangular and uses mode stirring or mode tuning technology to change the boundary conditions of the electromagnetic field so as to produce a statistically uniform field. To overcome the size and maintenance problems of the stirrers, it is proposed the use of diffusion metasurface in the RC to enhance the scattering. Such metasurface is much smaller than a stirrer [9]. According to the concept of coding metasurface, the designed 1-bit random coding metasurface (by employing the genetic algorithm) can provide an optimized distribution of unit cells to get a uniform backscattering (see **Figure 11**).

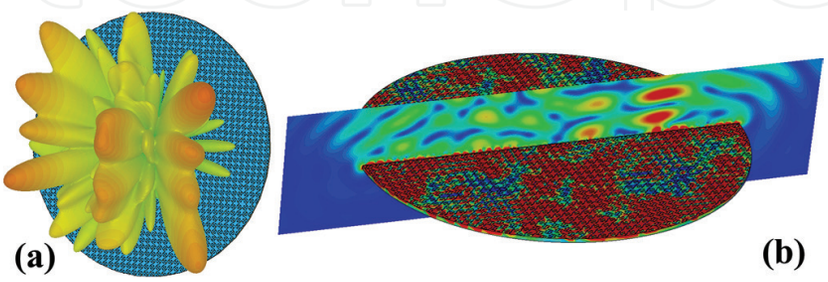

Figure 11. The 1-bit random coding diffusion metasurface distributions and simulated surface current distribution and near-field pattern under normal incidence. Reprinted with permission from Ref. [9]; Copyright 2018 Scientific Reports.

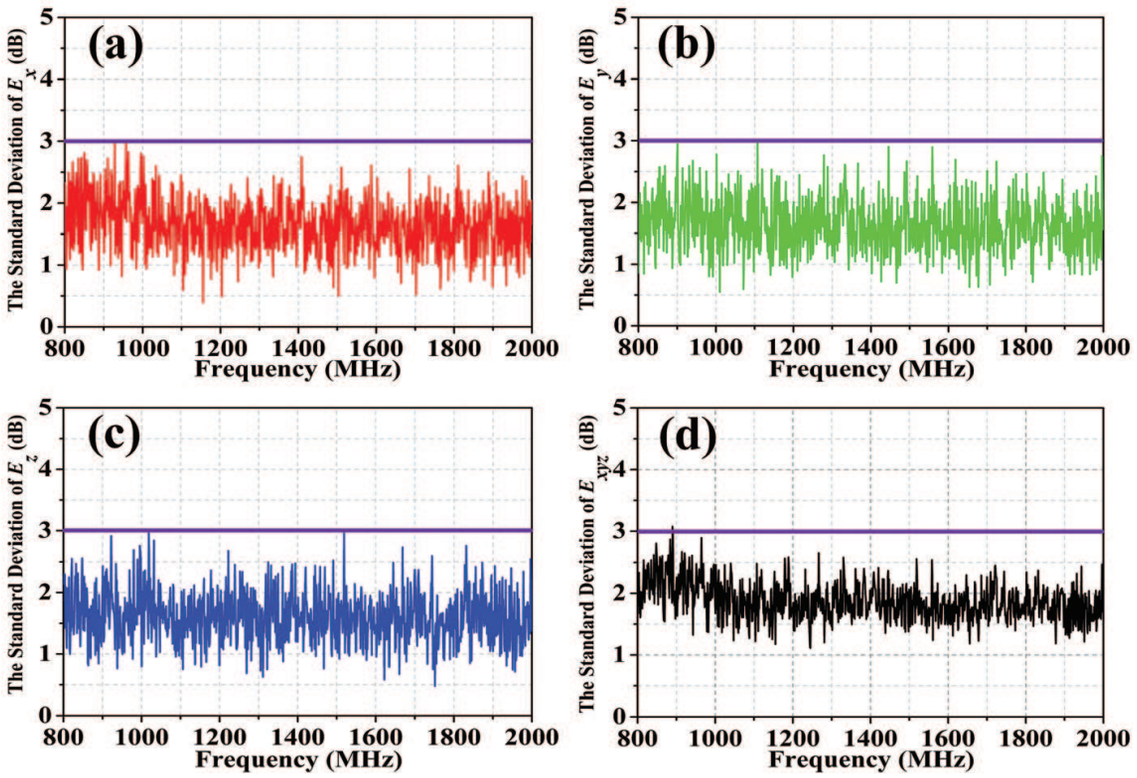

Figure 12. The standard deviations for the field uniformity of the test zone, which loaded the rotatable 1-bit random coding diffusion metasurface in the RC, and the purple lines are the tolerance requirements for the standard deviation of [10]. (a) the x-component, (b) the y-component, (c) the z-component, and (d) the combined of xyz components. Reprinted with permission from Ref. [9]; Copyright 2018 Scientific Reports.

When loaded the metasurface to the RC, it can act as a tuner. By setting the number of metasurface steps to 12, the standard deviation of the field is the one shown in **Figure 12**.

The results indicated that the rotatable 1-bit random coding diffusion metasurface can act as a tuner in the RC and it is of great interest as it shows that the metasurface on the wall increases the test zone available by avoiding the stirrer.

4. Conclusion and outlook

In this chapter, an overview of key metasurface concepts such as diffusion, anomalous reflection and refraction has been carried out, and their use in wavefront shaping and beamforming applications, followed by a discussion of polarization conversion in few-layer metasurfaces and their related properties have been discussed. An overview of diffusion coding metasurface reveals their ability to realize unique functionalities to reduce the radar cross-section. We also describe diffusion coding metasurfaces that can improve the field uniformity in reverberation chambers. Finally, we conclude by providing our opinions on opportunities and challenges in this rapidly developing research field. These works presented herein provide a glimpse of the opportunities available for advanced EM functional devices based on geometric phase coding metasurface, which may find applications in the future. Moreover,

scalability of these coding metasurfaces to frequencies in the range of THz or optical is possible, allowing for the controllability of reflection, and scattering of EM waves in these frequency domains [11].

Acknowledgements

The authors are grateful to National Natural Science Foundation of China (61,501,227, 61,071,019), Postdoctoral Science Foundation of China (2015 M581789), 56YAH17032 of NUAA, Jiangsu Innovation Program for Graduate Education (KYLX16–0370), Fundamental Research Funds for the Central Universities (NJ20160011), MINECO-Spain (TEC2016–75650-R), Generalitat de Catalunya (2017SGR-1159) and FEDER funds. Hengyi Sun acknowledges the China Scholarship Council (CSC) for Grant 201,706,830,064.

Conflict of interest

There is no conflict of interest.

Author details

Hengyi Sun[1,2]*, Changqing Gu[1], Zhuo Li[1] and Ferran Martin[2]

*Address all correspondence to: sunhy1123@nuaa.edu.cn

1 Key Laboratory of Radar Imaging and Microwave Photonics, Ministry of Education, College of Electronic and Information Engineering, Nanjing University of Aeronautics and Astronautics, Nanjing, China

2 CIMITEC, Departament d'Enginyeria Electrònica, Universitat Autònoma de Barcelona, Barcelona, Spain

References

[1] Yu N, Genevet P, Kats MA, Aieta F, Tetienne JP, Capasso F, Gaburro Z. Light propagation with phase discontinuities: Generalized laws of reflection and refraction. Science. 2011;**334**:333-337. DOI: 10.1126/science.1210713

[2] Della Giovampaola C, Engheta N. Digital metamaterials. Nature Materials. 2014;**13**:1115. DOI: 10.1038/nmat4082

[3] Moccia M, Liu S, Wu RY, et al. Coding metasurfaces for diffuse scattering: Scaling Laws, bounds, and suboptimal design. Advanced Optical Materials. 2017;**5**(19). DOI: 10.1002/adom.201700455

[4] Cui TJ, Qi MQ, Wan X, Zhao J, Cheng Q. Coding metamaterials, digital metamaterials and programmable metamaterials. Light: Science & Applications. 2014;**3**:e218. DOI: 10.1038/lsa.2014.99

[5] Sun H, Gu C, Chen X, Li Z, Liu L, Xu B, Zhou Z. Broadband and broad-angle polarization-independent metasurface for radar cross section reduction. Scientific Reports. 2017;**7**:40782. DOI: 10.1038/srep40782

[6] Sun H, Gu C, Chen X, Li Z, Liu L, Martín F. Ultra-wideband and broad-angle linear polarization conversion metasurface. Journal of Applied Physics. 2017;**121**:174902. DOI: 10.1063/1.4982916

[7] Sun H, Li Z, Chen X, Liu L, Xu B, Gu C. Realization of high-efficiency anomalous reflection using phase gradient metasurface at UHF. In: International Conference on Electromagnetics in Advanced Applications (ICEAA), 2016. 19-23 September 2016; Australia. Cairns: IEEE; 2016. pp. 435-437

[8] Dong X, Sun H, Gu C, Xu B, Wang K, Li Z. Reflective metasurface for generating vortex wave in ultra-wideband. In: 2018 IEEE International Symposium on Electromagnetic Compatibility and 2018 IEEE Asia-Pacific Symposium on Electromagnetic Compatibility; (EMC/APEMC); 14-17 May 2018. Singapore: IEEE; 2018

[9] Sun H, Li Z, Gu C, Xu Q, Chen X, Sun Y, Lu S, Martin F. Metasurfaced reverberation chamber. Scientific Reports. 2018;**8**:1577. DOI: 10.1038/s41598-018-20066-0

[10] Compatibility, Electromagnetic. Part 4-21: Testing and Measurement Techniques—Reverberation Chamber Test Methods. IEC Standard: 61000-4, 2003

[11] Chen K, Feng Y, Yang Z, et al. Geometric phase coded metasurface: From polarization dependent directive electromagnetic wave scattering to diffusion-like scattering. Scientific Reports. 2016;**6**:35968. DOI: 10.1038/srep35968